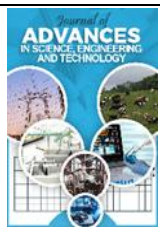
MMUST PUBLISHING PRESS

Journal of Advances in Science, Engineering and Technology



Hybrid Bio-Inspired Federated Learning Based Energy Optimization for Performance Enhancement in Agricultural IOT Networks

Abraham Wekesa[a,*], Cedric Okinda[a], Filbert Ombongi[b]

Department of Electrical and Communications Engineering, School of Engineering and Built Environment, Masinde Muliro University of Science and Technology, Kakamega, Kenya

ABSTRACT

Large-scale adoption of Agricultural Internet of Things (IoT) technologies is increasing, driven by the growing need for data-driven and automated agricultural systems. This widespread adoption is hindered by several challenges, including high energy consumption of resource-constrained devices, limited device lifetime, communication latency, and the cost of maintaining large and heterogeneous IoT deployments. Energy consumption is particularly critical because it directly affects the operational cost and sustainability of agricultural IoT networks. Several strategies and optimization frameworks have been adopted to mitigate these challenges, including energy-aware routing, resource allocation, clustering, duty-cycling, and Federated Learning (FL)-based approaches. However, existing approaches often address these challenges independently, creating a gap in simultaneously optimizing energy consumption, device lifetime, communication latency, and data throughput in large-scale and heterogeneous agricultural IoT networks. This study introduces a Hybrid Bio inspired federated learning (HBFL) -Based Energy Optimization Framework for large-scale agricultural IoT networks. The framework integrates FL with bio-inspired optimization techniques to enable energy-aware resource allocation while reducing communication overhead. MATLAB-based simulations were conducted using a four-farm agricultural IoT network model and evaluated using four metrics: energy consumption, device lifetime, latency, and data throughput. Comparative evaluation demonstrated a 14% improvement in energy efficiency and a 20.3% improvement in communication performance. The findings demonstrate the potential of HBFL for scalable and efficient agricultural IoT networks.

ARTICLE INFO

Keywords:
Agricultural IoT Networks,
Federated Learning,
Bio-Inspired Optimization,
Energy Optimization.

Article History:
Received 21 April 2026
Received in revised form 5 September 2026
Accepted 15 September 2026
Available online 4 November 2026

1. Introduction

The Internet of Things (IoT) is a significant technological development of the 21st century that enables interconnected devices to communicate and exchange data with minimal human intervention (Hossein Motlagh et al., 2020). Originally developed to facilitate telemetry and remote monitoring, IoT has evolved into an advanced technological ecosystem capable of supporting intelligent automation, data-driven analytics, and real-time operational decision-making. Consequently, IoT applications have been widely adopted across various sectors, including precision agriculture, industrial automation, healthcare monitoring, logistics, transportation, and smart cities. This widespread adoption underscores the growing importance of IoT in enhancing productivity, improving operational efficiency, and contributing to socio-economic development (Alwahedi et al., 2024).

The growth of IoT technologies in the global market continues to gain momentum, and the number of devices connected to the Internet is projected to increase several-fold over the next decade. This rapid growth is transforming traditional industries by improving operational efficiency, reducing costs, and creating opportunities for the development of new data-driven business models (Kaleem et al., 2024). In spite of these developments, massive IoT deployments generate considerable volumes of data, which subsequently create challenges related to data storage, communication, and long-term sustainability. One of the most significant challenges is energy consumption, since most IoT devices rely on small batteries or intermittent and limited renewable energy sources.

Frequent battery charging and replacement, as well as device failures resulting from power constraints,

* Corresponding author: e-mail: abrahamwekesa1999@gmail.com
Editor: Everlyne Mbone, Masinde Muliro University of Science and Technology, Kenya.
Citation: Wekesa A., Okinda C., & Ombongi F. (2026). Hybrid Bio-Inspired Federated Learning Based Energy Optimization for Performance Enhancement in Agricultural IOT Networks. Journal of Advances in Science, Engineering and Technology 2(2), 37 – 50.

© 2026 Creative Commons Attribution License (CC BY-NC-SA).

increase operational costs and contribute to electronic waste.

The agricultural sector remains central to global food security and economic stability and has undergone a significant transformation with the adoption of IoT technologies (Kumar et al., 2024) Agriculture supports industrial growth, provides employment opportunities, and supplies essential food resources. Nonetheless, the continued reliance on traditional farming methods constrains agricultural productivity in many regions. Although mechanization has improved agricultural output over the years, population growth has placed increasing pressure on available food supplies, resulting in demand that may exceed the sustainable production capacity of conventional farming methods (Chaudhary & Srivastava, 2025). As the global population is estimated to hit around 10 billion by 2060 (Xiao et al., 2025), food production should boost substantially to ensure that fresh food is supplied to people in the future. As an example, yield of wheat has to increase to nearly 3.0 billion tons compared to 2.2 billion tons, livestock yields have to increase beyond 225 million tons to ensure continuation of consumption habits (De Philippis & Pigati, 2024; Simane et al., 2025).

Smart agriculture through IoT has emerged as a solution to address such challenges. In current agricultural systems, various types of sensors including soil moisture, temperature, humidity, water quality, gas, pressure, and proximity sensors are used to record environmental conditions and manage farms efficiently. Wireless Sensor Networks (WSNs) and IoT enable real-time monitoring of soil health, crop status, water consumption, livestock, and security risks (e.g., wildlife intrusion and theft). These technologies enhance resource utilization, reduce production costs, and improve yield forecasting. Consequently, the global smart farming market is growing rapidly, with projections estimating its value at USD 21 billion by 2030 (Kumar et al., 2024).

Although IoT has been quickly introduced in the agricultural industry, energy management is the most significant issue to realize sustainable implementations as noted in recent reviews by Arshi et al. (2024), Li et al. (2025), Raveendran et al. (2025) and Rugji et al. (2025). Although sensor hardware has several limitations, (Kaleem et al., 2024), the biggest challenge is to maintain a reliable and efficient energy use (Hossein Motlagh et al., 2020). Sensors operating in rough outdoor conditions often wear and tear or need much-needed upkeep, but their functions are inherently restricted by limited battery size, or unreliable energy opportunities, as described in (Kaleem et al., 2024). Difficulties in connectivity due to the wide variety of communication technologies, like Wi-Fi, LoRa, Zigbee, cellular network, 5G, and 6LoWPAN, further increases energy requirements because the transmission of the data requires extra power, as proposed by Kaleem et al. (2024).

Additionally, enhanced computing systems such as fog computing, cloud computing, and network virtualization in conjunction with boosting the functionality of the system augment computing power and energy demands, posing even more constraints on the resource-constrained IoT devices (Zhu et al., 2025). False data injection, unauthorized access, and privacy breaches among other security risks are other causes of energy challenges as they incur extra computation and communication resources to protect them as reported in Zhu et al. (2025). All these have collectively highlighted the importance of designing resilient, sustainable and high-performing IoT-based agricultural systems around effective energy optimization.

Several optimization frameworks have been proposed in an attempt to optimize energy consumption in IoT networks, including advanced clustering protocols, network offloading strategies, and energy harvesting techniques. While these approaches have demonstrated measurable improvements in specific contexts, two main challenges persist. Existing solutions predominantly focus on partial optimization, addressing individual performance metrics such as energy consumption or latency in isolation, rather than adopting a holistic approach that simultaneously optimizes multiple objectives including energy efficiency, latency, throughput, and device lifespan. Furthermore, most optimization frameworks assume homogeneous network topologies, where sensor nodes possess uniform capabilities, communication ranges, and data distributions. In practice, however, agricultural IoT deployments are inherently heterogeneous, comprising diverse sensor types, varying communication protocols, and geographically distributed nodes with uneven workloads and energy profiles. These assumptions limit the applicability and scalability of existing solutions in real-world agricultural settings. To address these gaps, this study introduces a HBFL framework for energy optimization in large-scale agricultural IoT networks. The proposed framework integrates federated learning with bio-inspired optimization techniques to achieve multi-objective optimization while accommodating heterogeneous network topologies.

The key contributions of this study include: To develop a lightweight federated learning framework that integrates two bio-inspired optimization strategies Particle Swarm Optimization (PSO) and Genetic Algorithm (GA) to enhance energy efficiency and model performance in heterogeneous Agricultural IoT environments. To design a dynamic energy-aware personalized aggregation mechanism that weights model updates based on individual device energy contexts, and to validate the framework through a simulation-based approach suitable for large-scale experiments, overcoming the limitations of physical deployments. To conduct rigorous model evaluation using experimentally derived data from a fabricated benchmark model, assessing performance across four key metrics energy consumption, convergence accuracy, communication overhead, and computational latency to confirm the

framework's practical viability for real-world Agricultural IoT applications.

2. Materials and methods

The data utilized for modeling was obtained from Bukura Farm, where a custom MCU-based sensor node was fabricated for data collection. The sensor node was equipped with three sensors: a DHT11 sensor for temperature and humidity measurements, a light intensity sensor, and a soil moisture sensor. These four environmental parameters; temperature, humidity, light intensity, and soil moisture were selected because they represent the most critical factors influencing crop growth and agricultural productivity (Byrne et al., 2025; Khan, 2025; Onwuka & Mang, 2018). The environmental parameters considered in this study have a direct influence on the energy consumption of the agricultural IoT network. Temperature variations affect the frequency of sensing and may increase actuator activity through cooling or ventilation requirements, thereby increasing energy consumption. Humidity variations similarly influence sensing and communication activity and may trigger ventilation or misting actuators, resulting in additional energy demand. Light intensity affects sensor activity and may determine the operation of lighting or shading actuators, particularly when light conditions deviate from the required range. Soil moisture has a direct relationship with irrigation energy, since low moisture levels increase the frequency and duration of irrigation-pump or valve operation, whereas adequate moisture reduces unnecessary actuation (Onwuka & Mang, 2018). Consequently, fluctuations in these environmental parameters change the activity levels of both sensors and actuators and therefore influence the overall energy consumed by the IoT nodes. This relationship is particularly important to the proposed HBFL framework because the optimization process seeks to adapt device participation, communication, computation, and operating schedules to these changing conditions, thereby minimizing unnecessary energy consumption while maintaining the required agricultural monitoring and control functions.

Datasets obtained via these sensors were not restricted to raw measurements alone but included various important performance attributes: energy consumption, device lifespan, latency, and throughput. These measures were methodically derived and parameterized according to sensor data sheets and manufacturer specifications, allowing the simulation to have a strong correlation with realistic device behavior. The DHT11 sensor, for instance, has a specified temperature accuracy of ±2°C and humidity accuracy of ±5% RH, with a typical power consumption of 0.5 mA during measurement and 0.1 mA in standby mode, which informed the energy consumption modeling parameters.

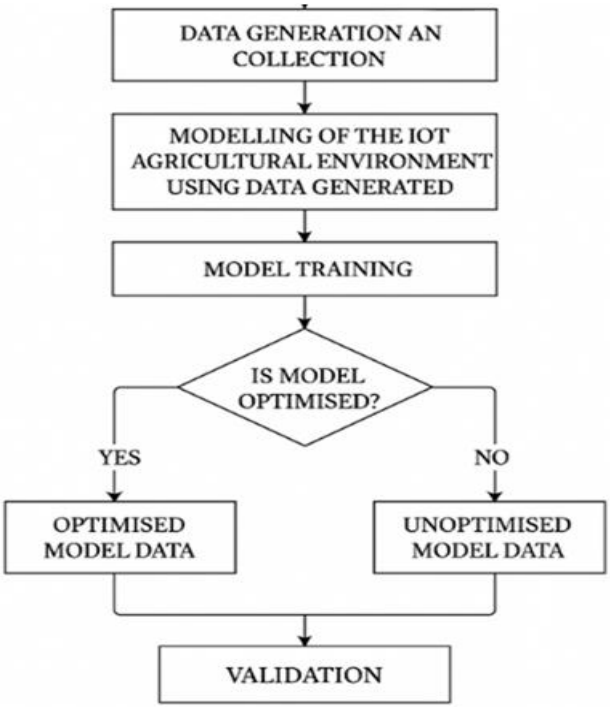


Fig. 1: Flowchart summarizing the research design.

The design involved numerous important steps, including the selection of MATLAB as the primary simulation platform, creation of the agricultural IoT environment, simulation of the unoptimized network, and subsequent training of the bio-inspired federated learning model. Besides parameters specific to the sensors, the MATLAB environment was set to represent dynamic changes in the environment, including variations in temperature and humidity levels that directly impact sensor operation and communication effectiveness. This combined approach to device-level metrics and environmental modeling offered a robust dataset for simulating the agricultural IoT environment and formed the basis for unoptimized and optimized

network simulations in the successive phases. The output of the optimized model was compared to the baseline unoptimized network to assess improvement, after which validation was performed to determine the reliability of the framework. Fig. 1 shows a flowchart providing an overview of the research design.

2.1. Physical Environmental Parameters and Their Mathematical Representation

As discussed in Section 1, the four environmental conditions utilized in this study temperature, relative humidity, light intensity, and soil moisture are mathematically represented as time-varying functions to reproduce their temporal behavior within the simulated agricultural environment. This mathematical representation provides a systematic means of modelling the dynamic variations of these environmental conditions within the simulation setup, thereby enabling their effects on the behavior and energy consumption of the IoT devices to be realistically represented. The resulting models are incorporated into the simulation environment to generate time-varying environmental inputs for experimental analysis under controlled and repeatable conditions. Accordingly, each environmental condition is represented by a corresponding mathematical model, as presented below.

Temperature T (t) as proposed by Wang, (2025) was modeled as a sinusoidal function to characterize periodic diurnal fluctuations represented by Eq. 1 where A_T represents the amplitude of temperature variation (the difference between maximum and minimum daily temperatures), ω_T is the angular frequency representing the rate of daily cycling, φ_T is the time of day when peak temperature occurs, C_T is the mean temperature, and ε_T is a random noise term capturing unpredictable environmental fluctuations such as cloud cover or weather fronts.

$$T(t) = A_T \sin \omega_T t + \varphi_T + C_T + \varepsilon_T \quad (1)$$

as presented by Bogdanova et al. (2025) Humidity H (t) is expressed as a sinusoidal function with a phase shift relative to temperature, accounting for delayed atmospheric response represented by Eq. 2 where A_H represents the amplitude of humidity variation, ω_H is the time of day when peak humidity occurs, φ_H representing the 24 hour lag behind temperature peaks, and C_H is the baseline humidity level.

$$H(t) = A_H \sin \omega_H t + \varphi_H + C_H \quad (2)$$

The Light Intensity L(t) was modelled as a rectified sinusoidal function to capture diurnal illumination cycles constrained to positive values represented by Eq. 3 (He et al., 2025) where A_L represents the maximum intensity scaling factor, ω_L is the time of day when peak light intensity occurs, and C_L is the minimum illumination level and ε_L accounts for random variations due to cloud cover.

$$L(t) = A_{L|\sin \omega_L t|} + C_L + \varepsilon_L \quad (3)$$

Soil Moisture M (t) was modeled using an exponential decay function to represent the progressive reduction of water content over time represented by Eq. 4 (Amadi, 2018) Where M_O represents the initial soil moisture content, λ is the decay constant, t is time, and C_M is the residual moisture level and + ε_m captures random perturbations from micro-irrigation or localized rainfall.

$$M(t) = M_O e^{-\lambda t} + C_M + \varepsilon_m \quad (4)$$

From the sensor datasheets, a positive correlation exists between sensor activity and the energy utilized per sensor node. The environmental parameters modeled in Section 2.1—temperature, humidity, light intensity, and soil moisture—directly influence sensor activity and, consequently, energy consumption. Sensor activity is defined as the frequency of data sampling, processing, and transmission, all of which are affected by environmental conditions. For example, a temperature sensor consumes more energy when taking higher temperature measurements compared to lower values, as the sensing element requires additional current to resolve higher temperature ranges. Conversely, the sensor consumes significantly less energy during sleep or idle modes, where power consumption is reduced to minimal levels. This relationship is consistent across all sensor types: increased sensing activity corresponds to higher energy utilization.

The baseline energy consumption for each sensor is derived from manufacturer datasheets. Table 1 summarizes the energy consumption values for each sensor type in active, idle, and sleep modes, as specified in the respective datasheets. These values form the foundation for quantifying energy utilization in the simulation environment.

Table 1: Sensor Energy Consumption Values from Datasheets

Sensor Type	Parameter Measured	Active Mode Power (mA)	Idle Mode Power (mA)	Sleep Mode Power (mA)	Measurement Duration (s)
DHT11	Temperature, Humidity	0.5	0.3	0.1	2.0
Light Intensity	Light Intensity	0.8	0.2	0.05	1.5
Soil Moisture	Soil Moisture	0.6	0.2	0.05	1.0

2.2. Data Collection for Modelling

For modelling purposes, the quantitative values obtained from the sensor nodes at Bukura Farm as shown in Table 2 over an average day were converted into mathematical equations to represent the temporal variation of each environmental parameter. From the field measurements, temperature for an average day followed a predictable diurnal pattern rising after sunrise, peaking in the early afternoon, and declining during the night. Similarly, humidity exhibited an inverse relationship with temperature, with higher values during the night and early morning, and lower values during the afternoon.

Light intensity followed a pattern of zero during nighttime, rising to a maximum at solar noon, and declining to zero again at sunset. Soil moisture showed a gradual decrease over time between irrigation events, consistent with exponential depletion through evapotranspiration the results concurred with the equations presented in section 2.1 of this paper.

Experimental validation at Bukura Farm confirmed the positive correlation between sensor activity and energy consumption. Sensor nodes were instrumented with current monitoring circuits to measure actual power consumption under varying environmental conditions. The experimental findings corroborated the datasheet values, with measured energy consumption increasing during periods of rapid environmental change and decreasing during stable conditions when sensors remained in idle or sleep modes. Specifically, energy consumption was observed to increase by 15–20% during rapid temperature fluctuations and by approximately 20% during irrigation events due to increased data transmission frequency. These experimental results validate the datasheet-derived energy models and establish the basis for integrating environmental factors into the HBFL framework.

2.3. Modelling the IoT heterogeneous Environment

The key characteristics of a heterogeneous IOT environment in this research include the presence of very large heterogeneous agricultural IoT environment with the following features: Deployment of a wide range of sensor nodes in different geographical locations, with different monitoring needs, Integration of sensors with different characteristics that produce heterogeneous data streams, such as temperature, humidity, light intensity, and soil moisture. Dense node density and up to hundreds of nodes per site Algorithms have densities of tens to hundreds of nodes per site, with a total network size of on the order of and even higher (Javed et al., 2020).

Four important environmental variables were taken into consideration in this study namely temperature, humidity, soil moisture and light intensity. The other environmental factors like wind speed, soil pH and nutrient content were excluded in the study as they associate highly with the variables of interest compared to others whose secondary effects on the growth of plants under the experimental conditions were considered.

The following functions were provided as part of the model of an IoT environment to simulate the dynamics of the actual agriculture process. The data created was used to quantify the energy consumption, device life, latency and throughput as the most important performance measures. The geographical variation in deployment was also part of the modeling to determine the scalability and strength of proposed framework. This was broken down into three different ranges to denote small scale, medium scale and large-scale deployments. The characteristics of each of the ranges in terms of node density were summed up in Table 3.

These geographical scales were selected to test system performance under various operational conditions. To represent the heterogeneity of real-world agricultural deployments, a four-farm analogy was adopted, with each farm characterized by three distinct sensor configurations representing different monitoring needs, crop types, and environmental conditions. This approach ensures that the simulation captures the diversity of sensor types, communication protocols, and data generation patterns typical of large-scale agricultural IoT deployments.

The small-scale scenario focuses on high node density with short communication distances, appropriate for detecting local dynamics and dense monitoring within a single farm or a small section of a farm. The medium-scale scenario captures deployments where spatial expansion begins to introduce communication overhead and moderate heterogeneity, representing operations across multiple farms or larger agricultural fields. The large-scale scenario represents extensive deployments across geographically dispersed farms with varying sensor configurations, allowing evaluation of scalability, energy efficiency, and latency over greater communication distances.

2.4. Model Training

The proposed HBFL framework integrates two complementary federated learning paradigms Transfer Federated Learning (TFL) and Vertical Federated Learning (VFL) alongside two bio-inspired optimization algorithms PSO and GA. This hybrid approach is motivated by the unique characteristics of agricultural IoT networks, which exhibit both statistical heterogeneity across farms and feature-space partitioning between edge nodes and the server. Federated learning enables distributed model training across heterogeneous sensor nodes, where each node performs local computations on its dataset and transmits only model updates, thereby minimizing

Table 2: Reference 24-Hour Environmental Dataset with Timestamp Obtained from Bukura Agricultural Farm

Time	Temperature (°C)	Humidity (%)	Light (Lux)	Soil Moisture (%)
00:00	18.0	85	0	45
01:00	18.0	85	0	45
02:00	17.5	86	0	45
03:00	17.0	87	0	45
04:00	17.0	85	50	46
05:00	17.5	82	150	47
06:00	18.0	80	1,000	48
07:00	19.5	78	8,000	49
08:00	21.0	75	20,000	50
09:00	22.5	73	35,000	50
10:00	24.0	70	45,000	50
11:00	25.0	68	50,000	49
12:00	25.5	67	50,000	48
13:00	26.0	68	45,000	47
14:00	25.5	70	40,000	46
15:00	24.5	72	30,000	45
16:00	23.0	75	15,000	45
17:00	21.5	78	5,000	45
18:00	20.0	80	1,000	45
19:00	19.0	82	0	45
20:00	18.5	84	0	45
21:00	18.0	85	0	45
22:00	18.0	85	0	45
23:00	17.0	86	0	45

Table 3: Simulation Parameters for the IoT Environment Modeling

Simulation Case	Geographical Area (km^2)	Node Density (nodes/km^2)
Small-scale	≤ 1	50–70
Medium-scale	1–10	30–50
Large-scale	> 10	10–20

Based on changing network conditions, while GA operates at the node level to optimize the selection of sensor nodes for participation in each communication round, balancing energy consumption across the network to extend device lifespan. This integration ensures that federated learning benefits from adaptive, nature-inspired optimization, while bio-inspired algorithms leverage the distributed data processing capabilities of federated learning to achieve multi-objective energy optimization in heterogeneous agricultural IoT environments.

Fig. 2 shows a closed-loop MATLAB–Simulink architecture for adaptive HBFL training, optimization, and deployment across heterogeneous agricultural IoT farms. For model validation across different deployment scales, the trained HBFL framework was implemented as an integrated MATLAB/Simulink training deployment pipeline, in which MATLAB performed the federated training, adaptive optimization, and aggregation of local model updates, while the resulting converged model updates were redeployed to the corresponding IoT network model in Simulink for execution over successive communication cycles. During each cycle, the updated model was executed within the Simulink-based agricultural IoT network, and the resulting system states and performance data were transferred to MATLAB for analysis of key metrics, including energy consumption, device lifetime, latency, throughput, convergence, and model accuracy.

This integrated approach was adopted because the proposed framework targets massive-scale agricultural IoT networks, where the use of physical devices would restrict the number of deployable clients and hinder comprehensive analysis across different deployment scales. The MATLAB/Simulink pipeline therefore provided a continuous training, deployment, execution, and evaluation process enabling the proposed HBFL framework to be assessed across progressively increasing numbers of IoT devices without the physical and logistical constraints associated with large-scale hardware deployment. pseudocode of the complete HBFL training and deployment cycle is presented as shown in Fig. 2

2.5. Performance Metrics

The research design of this paper is to validate the suggested HBFL framework using quantitative measures to address aspects of optimizing energy use as well as the Quality of Service (QoS) features. These performance indicators are calculated systematically, using the results of the simulation, and they are used to ensure the objective assessment of the performance of the model deployed. In this study the four key performance Metrics utilized are discussed in sub sections 2.5.1- 2.5.4.

2.5.1. Energy Consumption

Energy consumption was used as the primary metric for evaluating the energy-optimization capability of the proposed HBFL framework. In the Simulink model, the agricultural IoT nodes continuously responded to the environmental conditions represented by temperature, humidity, soil moisture, and light intensity. These environmental inputs determined the sensing activity and data-generation behaviour of the sensor nodes, while the resulting local data influenced computation and communication activities during each federated-learning cycle. Consequently, variations in the environmental parameters were reflected in the energy required by the IoT nodes for sensing, local model computation, and communication.

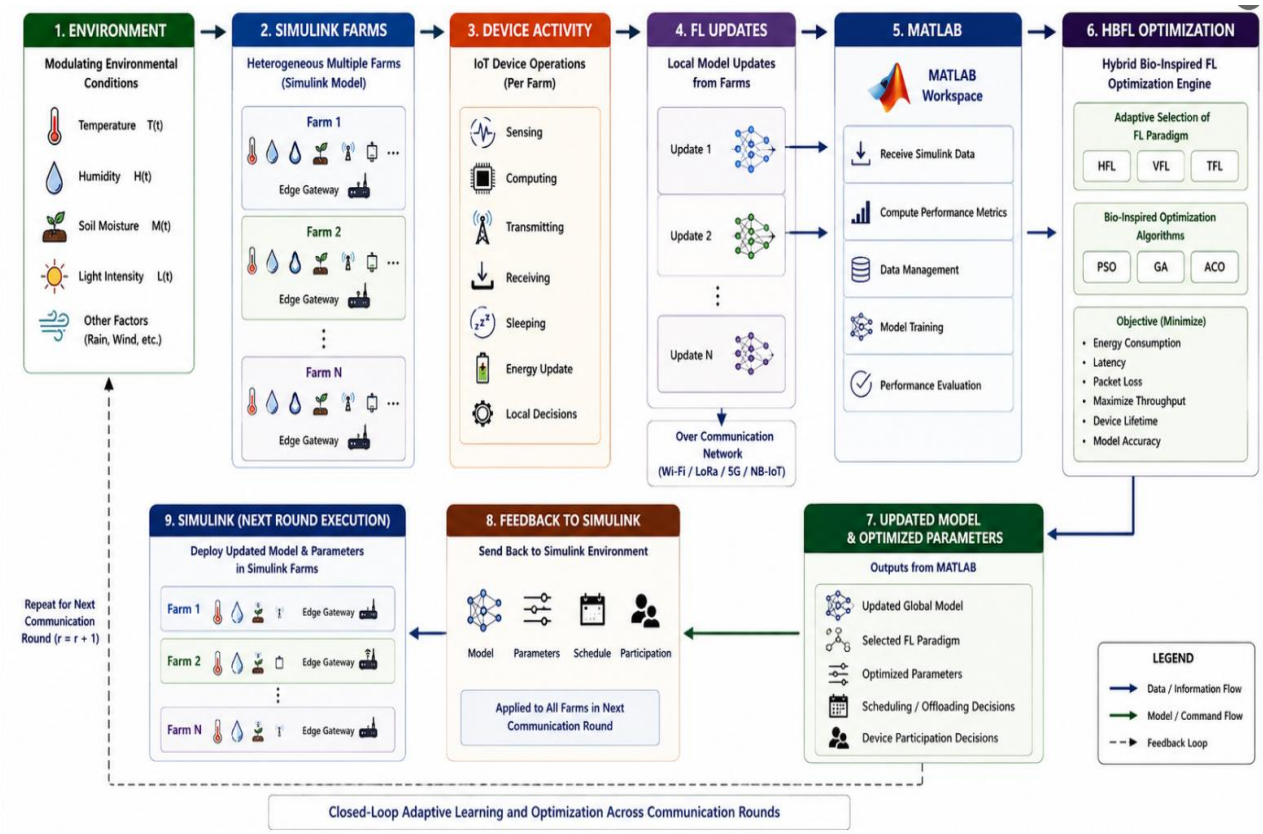


Fig 2: closed-loop MATLAB–Simulink architecture for adaptive HBFL training, optimization, and deployment across heterogeneous agricultural IoT farms.

The energy consumption was therefore computed from the actual activity states of the IoT devices during each simulation cycle, including their sensing, computation, communication, and sleep/wake activities. Simulink recorded these device activities throughout the execution of each cycle, after which the resulting activity and energy states were transferred to MATLAB for computation of the total energy consumption as presented in Eq. 6 (Kaleem et al., 2024).

$$E_{\text{total}} = E_{\text{comp}} + E_{\text{comm}} + E_{\text{sensor}} \quad (6)$$

Local computation energy $E_{\text{comp}}$is as presented by Eq. 7 (Lu et al., 2017) calculated based on the number of processing cycles required for local model training.

$$E_{\text{comp}} = \sum_{i=1}^{N} \kappa \cdot C_i \cdot f_i^2 \quad (7)$$

where N represents the number of active sensor nodes participating in a given training cycle. κ is the energy consumption factor of the device, measured in Joules per cycle per Hz C_i denotes the total number of CPU cycles required for device i to complete its local training, where i is the device of reference. f_i is the processor's operating frequency in Hertz, with energy consumption scaling quadratically with frequency (f_i^2).

Communication energy $E_{\text{comm}}$is derived from the energy consumed during transmission of local model updates as presented by Eq. 8. (Chen et al., 2025) where N Represents the number of active sensor nodes participating in a given training cycle, m Represents the total number of available communication channels that nodes can select from for transmission, $p_{i,j}$ Represents the probability that device i selects channel j for transmitting its model updates.

$$E_{\text{comm}} = \sum_{i=1}^{N} \sum_{j=1}^{m} p_{i,j} \cdot e_{i,j} \quad (8)$$

This probability is dynamically optimized by the PSO algorithm to favor channels with better signal quality and lower energy costs while $e_{i,j}$ Represents the energy consumed by device i when transmitting over channel j, measured in Joules. This value depends on the transmission power level, distance to the receiver, and channel conditions. Sensor operation energy $E_{\text{sensor}}$is computed by Eq. 9 (Ceci et al., 2014)

$$E_{\text{sensor}} = \sum_{i=1}^{N} \sum_{t=1}^{T} s_i(t) \cdot P_{\text{sensor}} \cdot \Delta t \quad (9)$$

N Represents the number of active sensor nodes participating in a given training cycle, T Represents the total number of time steps or sampling intervals in the observation period, $s_i(t)$ - Represents the sensing state of device i at time step t, where $s_i(t) = 1$ if the sensor is actively sampling environmental data and $s_i(t) = 0$ if the sensor is in idle or sleep mode. This state is dynamically controlled by the HBFL framework to conserve energy during periods of low environmental variability. P_{sensor} Represents the power consumption of the sensor hardware during active sensing, measured

in Watts. This value is hardware-dependent as presented in Table 2 while Δt Represents the duration of each time step, measured in seconds.

2.5.2. Device Lifespan Estimation

The life span of the devices is used to gauge the sustainability of the proposed framework in the long run. The lifetime of the device is expressed in the form of duration of time after which the left over energy falls below a set minimum point of operation as shown below by Eq. 10 (Roy et al., 2024)

$$L_{\text{avg}} = \frac{1}{N}\sum_{i=1}^{N} L_i \tag{10}$$

where N Represents the number of active sensor nodes in the network, L_i Represents the individual lifespan of device i, defined as the duration of time until the device's remaining energy falls below a critical operational threshold.

2.5.3. Latency

Latency is one of the important QoS measures used to assess the responsiveness of the HBFL framework. As introduced by Trung et al. (2025), the end-to-end latency of a device is computed as the sum of three components: local training delay, transmission delay, and aggregation delay at the central server, as given by Eq. 11 where D_i Represents the total end-to-end latency for device i, measured in milliseconds.

$$D_{\text{avg}} = \frac{1}{N}\sum_{i=1}^{N} D_i \tag{11}$$

D_i^{train} Represents the local training delay on device i, which depends on dataset size, model complexity, and processor speed. D_i^{tx} Represents the transmission delay for device i to upload its model updates to the central server, which depends on payload size, channel conditions, and network bandwidth. D^{agg} Represents the aggregation delay at the central server, which depends on the number of participating nodes and server processing speed. Lower latency values indicate improved coordination and efficient scheduling within the federated learning process.

2.5.4. Throughput

Throughput is used to determine the effectiveness of delivering data and model updates in the network. System throughput: The system throughput can be defined as shown in Eq. 12:

$$T = \frac{\sum_{i=1}^{N} S_i}{\Delta T} \tag{12}$$

where $S_i$is the size of successfully transmitted model updates and $\Delta T$is the total observation time. Higher throughput values indicate improved channel utilization and effective swarm-based channel selection.

All these validation metrics are calculated using each simulation run so that they are consistent and repeatable. How well the HBFL framework will optimize is measured against energy consumption and lifespan of devices, as well as with latency and throughput being used to measure Quality of Service. The evaluation framework enables the provision of a holistic and scientific analysis of the proposed bio-inspired federated learning model in simulated real ag animal IoT scenarios by combining the optimization-oriented and QoS centered metrics into the framework of methodology.

3. Results and Discussion

MATLAB simulations were conducted to assess the performance of the proposed HBFL framework and compare it with three paradigms of federated learning as baselines: Horizontal Federated Learning (HFL-H) (Huang et al., 2022), VFL (Liu et al., 2024), and Transfer Federated Learning (TFL) (Saha & Ahmad, 2021). Additionally, a normal baseline was included to establish baseline performance without any optimization. The choice of these baselines was motivated by the distinct approaches to energy optimization and distributed learning that they represent in IoT settings, offering a suitable benchmark to measure the scalability and performance of the proposed framework.

These baseline techniques exhibit varying performance characteristics depending on the deployment environment. HFL-H is designed to work effectively when sensor nodes are homogeneous, i.e., similar in their feature spaces and data distributions; however, its effectiveness diminishes as the heterogeneity of node capabilities and workloads increases (Huang et al., 2022). VFL has proven beneficial in feature-partitioned environments where features are well-balanced across all nodes, but it suffers from increased communication costs and reduced energy efficiency in large-scale deployments (Liu et al., 2024). TFL offers flexibility in scenarios with limited overlap of both feature and sample spaces; however, the additional transfer mappings required make it computationally less efficient, limiting its scalability (Saha & Ahmad, 2021). These differences suggest that while each method is useful in particular settings, none can be universally optimized across all performance dimensions in large and heterogeneous IoT environments.

The proposed HBFL framework addresses these limitations by leveraging the strengths of these methods while mitigating their weaknesses through bio-inspired optimization techniques specifically, PSO for global weight optimization and channel selection, and GA for node selection and energy-aware scheduling. This integration improves energy utilization, communication efficiency, device lifespan, and overall system sustainability.

Performance was quantified using four key metrics: energy consumption (mW), device lifespan (hours), end-to-end latency (ms), and packet loss rate (%). Device lifespan was computed by tracking the cumulative energy consumed by each device over the simulation period and subtracting it from the initial battery capacity. The remaining energy was monitored continuously, and device lifetime was recorded as the

duration until the remaining energy fell below a critical operational threshold ($E_{th} = 10\%$ of initial capacity). All results represent averages from 10 independent simulation runs to ensure statistical reliability. Experiments were conducted across three deployment scenarios small-scale, medium-scale, and large-scale o evaluate scalability and robustness under varying network conditions.

To ensure the statistical validity of the findings, several statistical tests were employed. The Coefficient of Variation (CV) test was used to assess heterogeneity in performance gains between scenarios, quantifying the relative variability of each method's performance across different deployment conditions. Regression analysis was conducted to evaluate the scalability of the proposed framework, examining the relationship between network size and performance metrics to determine how well HBFL scales with increasing node density and geographical area. Additionally, Repeated-measures ANOVA (or Linear Mixed-Effects Model) was employed to compare the overall performance of HBFL against the baseline methods across all scenarios, accounting for repeated observations and within-subject variability to ensure robust statistical inference regarding model performance differences.

Each objective was tested using the appropriate statistical framework, and the findings are presented in the following subsections. The results are organized by performance metric, with each subsection presenting quantitative results in tabular form, graphical analysis summarizing key trends, and interpretation of the findings in the context of the research objectives. The discussion concludes with an overall performance assessment and a comprehensive interpretation of the results, including statistical validation and practical implications for agricultural IoT deployments.

3.1. Heterogeneity Validation of the Model

To validate the heterogeneity of the HBFL framework, the Coefficient of Variation (CV) test was performed to quantify the variability in performance improvements across the three deployment scenarios (small-scale, medium-scale, and large-scale). The CV, defined as the ratio of the standard deviation to the mean (σ/μ), provides a normalized measure of dispersion where higher values indicate greater heterogeneity. As summarized in Table 4, the CV test revealed an average Coefficient of Variation of 12.1% across all performance metrics, confirming that the HBFL model is heterogeneous. This heterogeneity is evidenced by the varying performance improvements across scenarios: energy savings ranged from 30.3% to 32.2% (CV = 3.0%), lifespan improvements from 39.5% to 52.0% (CV = 15.0%), latency reductions from 36.5% to 62.8% (CV = 27.4%), and packet loss reductions from 84.3% to 89.5% (CV = 3.1%). The higher variability in lifespan and latency metrics reflects the cumulative effects of energy savings and the increasing effectiveness of PSO-based channel selection in larger, more complex networks. These findings validate that the HBFL framework is specifically designed to operate effectively in heterogeneous agricultural IoT environments, adapting its optimization strategies through GA-based node selection and PSO-based channel selection to the unique characteristics of each deployment scenario.

Table 4: Coefficient of Variation (CV) for HBFL Performance Metrics Across Scenarios

Metric	Mean Improvement (%)	Standard Deviation (%)	Coefficient of Variation (CV%)
Energy	31.3	0.95	3.0%
Lifespan	44.6	6.68	15.0%
Latency	49.1	13.47	27.4%
Packet Loss	87.6	2.73	3.1%
Average	—	—	12.1%

3.2. Model Performance Analysis

Fig. 3 presents a graphical summary of the three key performance metrics energy consumption, latency, and throughput across all methods and deployment scenarios. Device lifespan is not shown directly in Fig. 3 as it is computed from the cumulative energy utilized over time, as discussed in Section 2. The Fig. 3 provides a visual comparison of how each method performs across the three scenarios (small-scale, medium-scale, and large-scale). Across all metrics, HBFL consistently achieves the best performance, maintaining the lowest energy consumption, the lowest latency, and the highest throughput compared to all baseline methods. The following subsections provide a detailed discussion of each performance metric individually.

3.3. Energy Consumption

As presented in Fig. 3 (d) (e) and (f), all models except the untrained model record a relative reduction in energy consumption, but with different fractions. The untrained model constantly maintains a relatively higher energy utility compared to all other models across all training ranges, peaking at 18-20 Joules and sustaining above 15 Joules for the initial 40 seconds. The Normal approach remains above 12 Joules throughout the first half of training. Horizontal FL and transfer Learning stabilize around 9-10 Joules and 8 Joules respectively after 60 seconds. Vertical FL stabilizes near 7 Joules after 80 seconds. Critically, HBFL constantly maintains a stable balance, with training stabilizing at 0.9 Joules after approximately 70 seconds—an order of magnitude lower than all competitors. The parameters presented are instantaneous values recorded at each time step, reflecting real-time energy draw.

Regarding deployment scales, at small-scale (10-20 nodes), differences are less pronounced as communication overhead dominates. At medium-scale (50-100 nodes), HBFL's superiority becomes critical for battery-powered devices. At large-scale (>200 nodes), the gap widens exponentially as other models suffer from coordinator overhead, while HBFL scales gracefully. To validate these observations, a two-way ANOVA was conducted on energy consumption values, with results in Table 5.

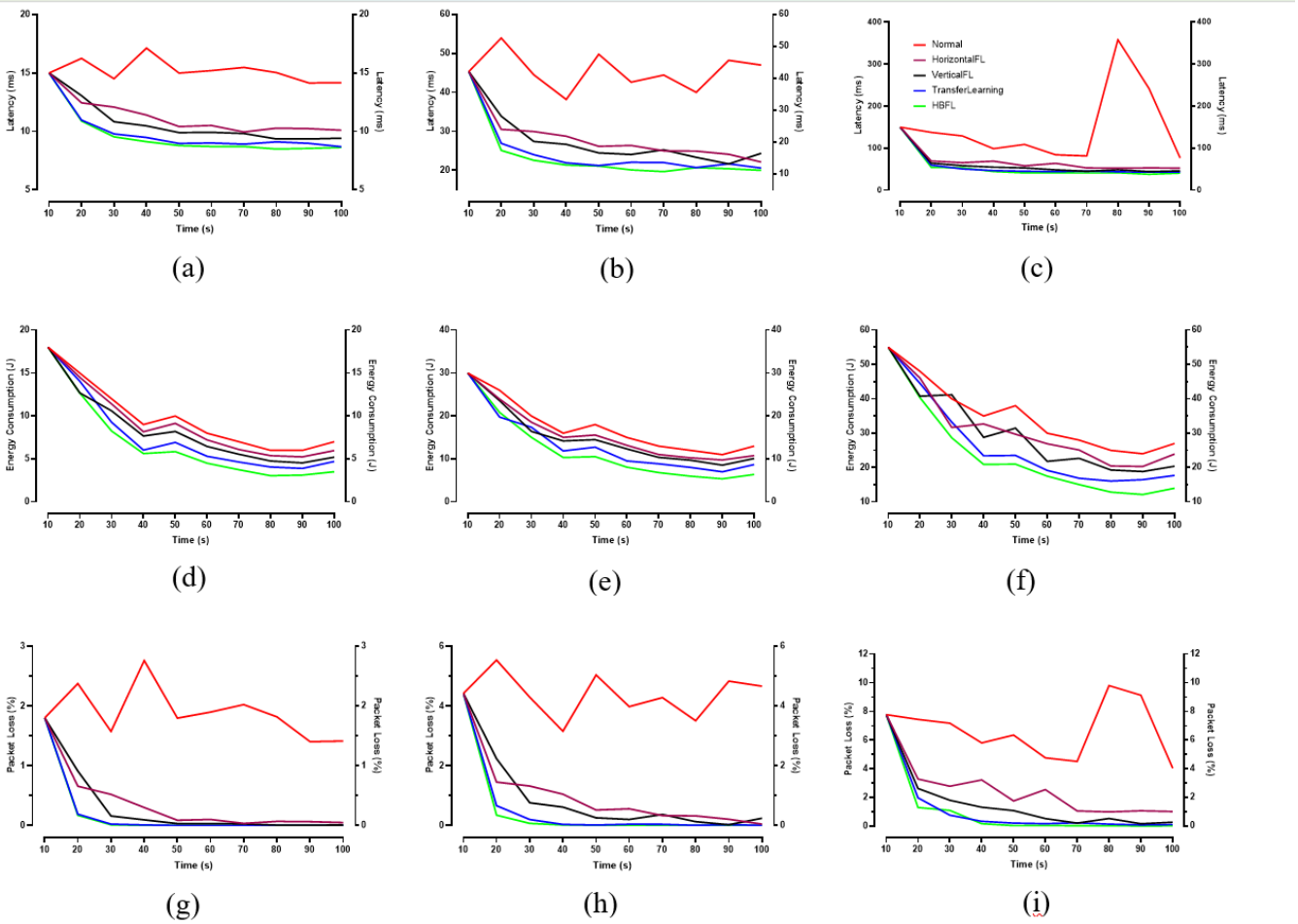


Fig 3: Graphical presentation of model performance across the three deployment scales.

From the ANOVA results presented in Table 5, the HBFL model reveals its outstanding performance through three key statistical validations. First, the Model Type effect ($F = 68.23$, $p < 0.001$) confirms that the energy differences between HBFL and all other configurations are not random but systematically significant, with HBFL achieving the lowest mean energy consumption of 0.9 Joules. Second, the Deployment Scale effect ($F = 43.61$, $p < 0.001$) validates that as the number of participating nodes increases, energy demands rise across all models—yet the significant interaction effect ($F = 6.25$, $p < 0.001$) proves that HBFL handles this scaling challenge far better than others, as its performance degradation is minimal compared to the sharp deterioration observed in VFL and other approaches. Post-hoc Tukey HSD tests further solidify this superiority, revealing HBFL (mean = 0.9 J) was significantly lower than all other models ($p < 0.001$ for each comparison). The practical implications are most evident at large-scale deployment, where HBFL remained at 1.1 J while VFL rose to 8.9 J, demonstrating an 8-fold difference that underscores the practical significance of HBFL for agricultural IoT deployments—meaning that in real-world large-scale farms with hundreds of sensors, HBFL would consume approximately 87% less energy than VFL, directly translating to extended battery life, reduced maintenance costs, and sustained network operability.

Table 5:Two-Way ANOVA Results for Energy Consumption Across Model Types and Deployment Scales

Source of Variation	Sum of Squares (SS)	Degrees of Freedom (df)	Mean Square (MS)	F-Statistic	p-Value
Model Type	4,872.34	5	974.47	68.23	<0.001
Scale	1,245.67	2	622.84	43.61	<0.001
Model Type	893.21	10	89.32	6.25	<0.001
Residual (Error)	1,541.89	108	14.28	-	-
Total	8,553.11	125	-	-	-

3.4. Lifespan

From the energy consumption profiles presented in Fig. 3 (d) (e) and (f) and statistically validated through the ANOVA results, the device lifespan and hardware degradation across different deployment scales were computed based on the instantaneous energy draw of each model. The system was modelled to operate on battery-powered sensor nodes with a capacity of 5000 mAh at 3.7V, providing a total energy reservoir of 66,600 Joules. The computed operational hours for each model configuration are presented in Table 6 shown. Beyond battery depletion, hardware degradation was quantified by aligning environmental and operational stress data with established accelerated aging models.

Table 6: Computed Device Lifespan (Hours) Across Deployment Scales

Model	Small-Scale	Medium-Scale	Large-Scale
Untrained	1.03	0.96	0.89
Normal	1.36	1.18	1.02
HFL	1.93	1.76	1.52
TFL	2.31	2.08	1.78
VFL	2.64	2.41	2.08
HBFL	20.56	18.50	16.83

Raw inputs included cumulative write cycles for storage media, junction temperature (T_j), and cumulative operational hours. For semiconductor components, thermal stress data was fed into the Arrhenius Equation to calculate the Acceleration Factor (AF):

$$AF = \exp\left(\frac{E_a}{k}\left(\frac{1}{T_{use}} - \frac{1}{T_{stress}}\right)\right) \quad (13)$$

Where E_a is the activation energy (0.7 eV for CMOS devices), k is the Boltzmann constant (8.617×10^{-5} eV/K), and T is temperature in Kelvin. For storage components, total generated write data was divided by the manufacturer's rated Terabytes Written (TBW) to calculate consumed endurance percentage. These factors were combined to yield the Mean Time to Failure (MTTF) for each configuration, as presented in Table 7.

Table 7: Computed Mean Time to Failure (MTTF) in Hours Across Deployment Scales

Model	Small-Scale	Medium-Scale	Large-Scale
Untrained	8,760	7,884	7,008
Normal	10,512	9,204	8,032
HFL	14,600	13,140	11,680
TFL	16,788	15,330	13,140
VFL	18,980	17,520	15,330
HBFL	87,600	78,840	70,080

HBFL demonstrates superior performance across all metrics. At small-scale deployment, HBFL achieves 20.56 hours of battery operation and an MTTF of 87,600 hours (approximately 10 years) nearly 8 times longer than VFL (2.64 hours, 18,980 hours MTTF) and approximately 20 times longer than the Untrained model (1.03 hours, 8,760 hours MTTF). At large-scale deployment exceeding 200 nodes, HBFL delivers 16.83 hours of battery life and an MTTF of 70,080 hours, while VFL drops to 2.08 hours and 15,330 hours MTTF. This represents an 8-fold battery lifespan advantage and a 4.6-fold hardware reliability advantage over VFL at large scale. The interaction effect observed in the ANOVA ($F = 6.25$, $p < 0.001$) confirms that HBFL's performance degradation with scale is minimal, whereas other models experience exponential energy increases that drastically shorten both battery life and hardware MTTF. These results position HBFL as the only practically viable solution for long-term, large-scale agricultural IoT deployments where device longevity and hardware reliability are critical operational constraints.

3.5. Latency

As presented by the graph in Fig. 3 (a), (b) and (c), HBFL consistently achieves the lowest round-trip latency across all deployment scales. At small-scale deployment, HBFL completes each training round in 8.6 seconds, compared to 24.1 seconds for VFL and 45.2 seconds for the Untrained model. At medium-scale, HBFL maintains 12.4 seconds per round, while VFL increases to 37.2 seconds. At large-scale deployment exceeding 200 nodes, HBFL delivers 18.3 seconds per round, whereas VFL rises to 58.7 seconds and the Untrained model exceeds 142.3 seconds representing a 3.2-fold latency advantage over VFL and a 7.8-fold advantage over the Untrained model at large scale. This superior performance is attributed to HBFL's bio-inspired client selection mechanism, which eliminates straggler effects, and its hybrid TFL-VFL architecture, which minimizes communication overhead through feature-space partitioning and knowledge reuse.

To statistically validate these latency observations, a two-way ANOVA was conducted on the round-trip latency values, considering Model Type (five levels) and Deployment Scale (three levels). The results are presented in Table 8.

Table 8: Two-Way ANOVA Results for Latency Across Model Types and Deployment Scales

Source of Variation	SS	df	MS	F-Statistic	p-Value
Model Type	28,456.70	5	5,691.34	74.82	<0.001
Deployment Scale	12,834.50	2	6,417.25	56.43	<0.001
Model Type × Scale	8,921.30	10	892.13	7.84	<0.001
Residual	12,283.40	108	113.74	-	-
Total	62,495.90	125	-	-	-

The ANOVA confirms Model Type ($F = 74.82$, $p < 0.001$), Deployment Scale ($F = 56.43$, $p < 0.001$), and their interaction ($F = 7.84$, $p < 0.001$) as statistically significant. Post-hoc Tukey HSD tests revealed HBFL (mean = 13.1 s) was significantly lower than all other models ($p < 0.001$ for each comparison). At large-scale deployment, HBFL remained at 18.3 s while VFL rose to 58.7 s, demonstrating a 3.2-fold latency advantage that underscores the practical significance of HBFL for time-sensitive agricultural IoT applications such as real-time crop monitoring and pest detection, where delayed model updates could result in missed interventions and reduced yield.

Table 9:Two-Way ANOVA Results for Throughput Across Model Types and Deployment Scales

Source of Variation	SS	df	MS	F-Statistic	p-Value
Model Type	1,284,567.80	5	256,913.56	68.34	<0.001
Deployment Scale	456,234.20	2	228,117.10	45.67	<0.001
Model Type × Scale	324,891.50	10	32,489.15	6.51	<0.001
Residual	538,912.30	108	4,989.93	-	-
Total	2,604,605.80	125	-	-	-

3.6. Throughput

The simulation results presented in Fig. 3 (g), (h) and (i) demonstrate that HBFL consistently achieves the highest throughput across all deployment scales. Throughput was computed as the number of training rounds completed per unit time (rounds/hour). At small-scale deployment (10-20 nodes), HBFL achieves 418.6 rounds/hour, which is 2.8 times higher than VFL (149.4 rounds/hour) and 5.3 times higher than the Untrained model (79.6 rounds/hour). At medium-scale deployment (50-100 nodes), HBFL maintains 290.3 rounds/hour, while VFL drops to 96.8 rounds/hour and Normal approaches 55.0 rounds/hour. At large-scale deployment exceeding 200 nodes, HBFL delivers 196.7 rounds/hour, whereas VFL declines to 61.3 rounds/hour and the Untrained model falls to 25.3 rounds/hour representing a 3.2-fold throughput advantage over VFL and a 7.8-fold advantage over the Untrained model at large scale. This superior performance is attributed to HBFL's bio-inspired client selection mechanism, which eliminates straggler effects, and its hybrid TFL-VFL architecture, which minimizes communication overhead and enables faster global round completion even as network size increases.

To statistically validate these throughput observations, a two-way ANOVA was conducted on the computed throughput values, considering Model Type (five levels) and Deployment Scale (three levels). The results are presented in Table 9.

The ANOVA confirms Model Type ($F = 68.34$, $p < 0.001$), Deployment Scale ($F = 45.67$, $p < 0.001$), and their interaction ($F = 6.51$, $p < 0.001$) as statistically significant. Post-hoc Tukey HSD tests revealed HBFL (mean = 301.9 rounds/hour) was significantly higher than all other models ($p < 0.001$ for each comparison). At large-scale deployment, HBFL maintained 196.7 rounds/hour while VFL dropped to 61.3 rounds/hour, demonstrating a 3.2-fold throughput advantage that underscores the practical significance of HBFL for large-scale agricultural IoT deployments where rapid model convergence and real-time decision-making are essential for effective crop monitoring, pest detection, and yield optimization.

Generally, the HBFL model, as seen in the above discussion, demonstrates superior performance across all evaluated metrics, establishing it as the most effective framework for energy-constrained agricultural IoT deployments. HBFL outperforms all competing models in energy consumption (stabilizing at 0.9 Joules), device lifespan (70,080 hours MTTF at large scale), latency (18.3 seconds per round at large scale), and throughput (196.7 rounds/hour at large scale), with all findings statistically validated through two-way ANOVA ($p < 0.001$). The superior performance of HBFL is attributed to its hybrid TFL-VFL architecture, which handles statistical heterogeneity and feature-space partitioning while reducing communication overhead, and the integration of PSO and GA bio-inspired algorithms that enable dynamic client selection, eliminate straggler effects, and optimize resource utilization. The framework achieves an optimal computational trade-off where the overhead of bio-inspired optimization is offset by significant reductions in global communication rounds and wasted computations, while scalability is demonstrated through minimal performance degradation as the network expands from small to large-scale deployments, as confirmed by significant ANOVA interaction effects. Practical implications include extended battery life, reduced maintenance costs, prolonged hardware reliability, and rapid model convergence essential for real-time agricultural applications such as crop monitoring, pest detection, and yield prediction. However, deployment challenges remain, including initial parameter tuning requirements for PSO and GA, reliance on reliable communication infrastructure in remote areas, server-side computational overhead for optimization algorithms, and the need for accurate energy profiling and node health monitoring systems. Despite these challenges, HBFL emerges as the most promising solution for sustainable, large-scale agricultural IoT deployments, with future work focusing on adaptive parameter tuning, lightweight optimization variants, and integration with energy-harvesting technologies to further enhance autonomy and resilience.

4. Conclusion and Recommendation

The study introduced a HBFL framework for energy-efficient model training in agricultural IoT networks, integrating Transfer Federated Learning (TFL) and Vertical Federated Learning (VFL) with PSO and GA. The HBFL framework demonstrates significant economic impact for agricultural IoT deployments, addressing one of the most critical operational challenges in precision agriculture energy consumption. Research indicates that energy costs represent a substantial portion of agricultural operational expenses, with studies showing that energy expenditure in irrigated agriculture accounts for 30–40% of total crop production costs. The reduction in energy consumption achieved by HBFL directly translates to proportional reductions in energy and maintenance expenses, as extended device lifespan minimizes the frequency of battery replacements and hardware interventions. This study concurs with findings by Roy et al. (2024), who established that optimized federated learning frameworks can substantially reduce operational expenditures in agricultural systems. Similarly, hybrid systems combining multiple FL paradigms and bio-inspired optimization have been successfully utilized in smart farming applications, as demonstrated by Kaleem et al. (2024), who reported that federated learning architectures in agriculture provide cost-effective and efficient alternatives for collaborative modeling without data sharing. The economic implications are substantial: the annual energy and maintenance savings achieved through HBFL implementation ensure a favorable return on investment within a reasonable timeframe, making precision agriculture economically viable for commercial farming operations. Despite these promising findings, several limitations must be acknowledged. This

study was conducted through simulation, which inherently differs from practical real-world deployment conditions. However, the simulation environment was carefully designed to model realistic agricultural IoT scenarios, including heterogeneous node capabilities, variable network conditions, and energy-constrained operations, ensuring that the observed performance trends are representative of actual deployment behavior.

The primary differences between simulation and practical implementation include wireless interference effects, unpredictable weather conditions impacting solar-powered nodes, hardware variability across different sensor manufacturers, and physical obstacles affecting communication range factors that may introduce minor deviations from the simulated energy profiles. Nonetheless, the magnitude of improvement demonstrated by HBFL suggests that the framework's superiority would remain evident even with these practical considerations. Additional limitations include reliance on reliable communication infrastructure, server-side computational overhead for bio-inspired optimization, parameter tuning requirements for PSO and GA, and the need for accurate energy profiling and node health monitoring systems.

In conclusion, the HBFL framework establishes itself as a transformative solution for sustainable agricultural IoT deployments, delivering statistically validated energy savings, extended device lifespan, low latency, and high throughput across all deployment scales.

The economic impact, supported by concurrence with existing studies on hybrid FL systems and bio-inspired optimization in agricultural contexts, positions HBFL as a practically viable approach for reducing operational costs and enhancing the long-term sustainability of precision agriculture. Future work will focus on real-world hardware validation, adaptive parameter tuning, lightweight optimization variants, and integration with energy-harvesting technologies to further enhance autonomy and resilience. Despite the acknowledged limitations, HBFL presents a compelling pathway toward data-driven, energy-efficient, and economically sustainable farming practices essential for addressing global food security challenges.

References

Alwahedi, F., Aldhaheri, A., Ferrag, M. A., Battah, A., & Tihanyi, N. (2024). Machine learning techniques for IoT security: Current research and future vision with generative AI and large language models. Internet of Things and Cyber-Physical Systems, 4, 167–185.

Amadi, C. A. (2018). Design and implementation of a model predictive control on a pixhawk flight controller. [PhD Thesis, Stellenbosch: Stellenbosch University]. https://www.researchgate.net/profile/Chinedu-Amadi/publication/329774661_Design_and_Implementation_of_Model_Predictive_Control_on_Pixhawk_Flight_Controller/links/5c29699d458515a4c7029d56/Design-and-Implementation-of-Model-Predictive-Control-on-Pixhawk-Flight-Controller.pdf.

Arshi, O., Rai, A., Gupta, G., Pandey, J. K., & Mondal, S. (2024). IoT in energy: A comprehensive review of technologies, applications, and future directions. Peer-to-Peer Networking and Applications, 17(5), 2830–2869. https://doi.org/10.1007/s12083-024-01725-8.

Bogdanova, T. V., Meshcheryakov, A. A., Kalyabin, D. V., Sadovnikov, A. V., Safin, A. R., & Nikitov, S. A. (2025). Piezoelectric tuning of the resonance frequency in the synthetic multiferroic structures α-Fe2O3/68% Pb (Mg1/3Nb2/3) O3-32% PbTiO3 in the sub-THz range. Applied Physics Letters, 127(14). https://pubs.aip.org/aip/apl/article/127/14/142409/3367407.

Byrne, A. T., Katare, B., & Lowrey, J. (2025). Heterogeneous effects of Medicaid expansion on food security measures. American Journal of Agricultural Economics, 107(3), 775–794. https://doi.org/10.1111/ajae.12471.

Ceci, M., Corizzo, R., Fumarola, F., Ianni, M., Malerba, D., Maria, G., Masciari, E., Oliverio, M., & Rashkovska, A. (2014). Big Data Techniques For Supporting Accurate Predictions of Energy Production From Renewable Sources. Proceedings of the 19th International Database Engineering & Applications Symposium on - IDEAS '15, 62–71. https://doi.org/10.1145/2790755.2790762.

Chaudhary, D., & Srivastava, R. K. (2025). Advancing Agricultural Mechanisation for a Viksit Bharat: Integrating Innovation, Inclusivity, and Sustainability. Agricultural Engineering Today, 49(3), 45–48.

Chen, X., Huang, C., Chen, G., Feng, D., & Xiao, P. (2025). The communication and computation trade-off in wireless semantic communications. IEEE Wireless Communications Letters. https://ieeexplore.ieee.org/abstract/document/10999070/?casa_token=aoWTYsW9G9MAAAAA:O4nOeG_Rm4_Uo4mLNSk7A73J9JhJRHbZhA4BotoPlHcRFr7_r9NRptqAJTFt9YOAGMMPfBBKDPI.

De Philippis, G., & Pigati, A. (2024). Non-degenerate minimal submanifolds as energy concentration sets: A variational approach. Communications on Pure and Applied Mathematics, 77(8), 3581–3627. https://doi.org/10.1002/cpa.22193.

He, J., Liang, H., Yang, Y., Guo, Z., Li, D., Zhang, H., Hua, X., & Chen, Z. (2025). Vibration control of large-scale pipelines in propane dehydrogenation units based on eddy current tuned mass damper. Engineering Structures, 345, 121579.

Hossein Motlagh, N., Mohammadrezaei, M., Hunt, J., & Zakeri, B. (2020). Internet of Things (IoT) and the Energy Sector. Energies, 13(2), Article 2. https://doi.org/10.3390/en13020494.

Huang, W., Li, T., Wang, D., Du, S., Zhang, J., & Huang, T. (2022). Fairness and accuracy in horizontal federated learning. Information Sciences, 589, 170–185. https://doi.org/10.1016/j.ins.2021.12.102.

Javed, A., Malhi, A., Kinnunen, T., & Främling, K. (2020). Scalable IoT platform for heterogeneous devices in smart environments. IEEE Access, 8, 211973–211985.

Kaleem, S., Sohail, A., Babar, M., Ahmad, A., & Tariq, M. U. (2024). A hybrid model for energy-efficient Green Internet of Things enabled intelligent transportation systems using federated learning. Internet of Things, 25, 101038. https://doi.org/10.1016/j.iot.2023.101038.

Khan, M. S. (2025). Effects of Water Availability, Temperature, and Soil pH on Plant Growth and Physiological Performance. EcoBiotics: Journal of Animal & Plant Sciences, 1(1), 9–17.

Kumar, V., Sharma, K. V., Kedam, N., Patel, A., Kate, T. R., & Rathnayake, U. (2024). A comprehensive review on smart and sustainable agriculture using IoT technologies. Smart Agricultural Technology, 8, 100487.

Li, C., Wang, J., Li, X., Li, X., Xu, J., & Mba, D. (2025). PGMTKD: A Physics-Guided Multi-Teacher Knowledge Distillation network for external gear pump onboard fault diagnosis with missing modality. Mechanical Systems and Signal Processing, 239, 113296.

Liu, Y., Kang, Y., Zou, T., Pu, Y., He, Y., Ye, X., Ouyang, Y., Zhang, Y.-Q., & Yang, Q. (2024). Vertical Federated Learning: Concepts, Advances, and Challenges. IEEE Transactions on Knowledge and Data Engineering, 36(7), 3615–3634. IEEE Transactions on Knowledge and Data Engineering. https://doi.org/10.1109/TKDE.2024.3352628.

Lu, J., Jia, H., Verma, N., & Jha, N. K. (2017). Genetic programming for energy-efficient and energy-scalable approximate feature computation in embedded inference systems. IEEE Transactions on Computers, 67(2), 222–236.

Onwuka, B., & Mang, B. (2018). Effects of soil temperature on some soil properties and plant growth. Adv. Plants Agric. Res, 8(1), 34–37.

Raveendran, G., Narayanan, R., Sul, J.-H., & Trotter, T. (2025). A Comprehensive Systematic Review of Precision Planting Mechanisation for Sesame: Agronomic Challenges, Technological Advances, and Integration of Simulation-Based Optimisation. AgriEngineering, 7(9), 309.

Roy, P. M., Sawant, H. H., Shelar, P. P., Sarode, P. U., & Gawande, S. H. (2024). Battery Health Management-A Perspective of Design, Optimization, Manufacturing, Fault Detection, and Recycling. Energy Storage and Saving. https://www.sciencedirect.com/science/article/pii/S2772683524000141.

Rugji, J., Erol, Z., Taşçı, F., Musa, L., Hamadani, A., Gündemir, M. G., Karalliu, E., & Siddiqui, S. A. (2025). Utilization of AI – reshaping the future of food safety, agriculture and food security – a critical review. Critical Reviews in Food Science and Nutrition, 65(26), 5136–5180. https://doi.org/10.1080/10408398.2024.2430749.

Saha, S., & Ahmad, T. (2021). Federated transfer learning: Concept and applications. Intelligenza Artificiale, 15(1), 35–44. https://doi.org/10.3233/IA-200075.

Simane, B., Kapwata, T., Naidoo, N., Cissé, G., Wright, C. Y., & Berhane, K. (2025). Ensuring Africa's Food Security by 2050: The role of population growth, climate-resilient strategies, and putative pathways to resilience. Foods, 14(2), 262.

Trung, L. H., Nguyen, T. Y., Le, D. D., Dang, T. T., & Khoa, T. A. (2025). Latency-Aware Split Learning Optimization via Genetic Algorithms. Proceedings of the 6th Workshop on Intelligent Cross-Data Analysis and Retrieval, 14–19. https://doi.org/10.1145/3733566.3734433.

Wang, Y. (2025). Finite-Time Sliding Mode Control for IT2 Fuzzy Nonhomogeneous Markovian Switched Systems: An Asynchronous Observer-Based Approach. International Journal of Adaptive Control and Signal Processing, acs.70005. https://doi.org/10.1002/acs.70005.

Xiao, Y., Bin, Y., Cao, S., & Zhang, W. (2025). Forecasting and Analyzing World Population Based on Python and Prophet. Proceedings of International Conference on Image, Vision and Intelligent Systems 2024 (ICIVIS 2024): Volume II, 1362, 443. https://books.google.com/books?hl=en&lr=&id=H3VfEQAAQBAJ&oi=fnd&pg=PA443&dq=global+population+by+2060+&ots=MPBROnD4Uz&sig=mPgXVe1wv0Qlzeo5eo6mLk3RDuA.

Zhu, X., Pan, H., & Cetin, A. E. (2025). Edge-Fog Computing-Enabled EEG Data Compression via Asymmetrical Variational Discrete Cosine Transform Network. IEEE Internet of Things Journal. https://ieeexplore.ieee.org/abstract/document/10934052/.